Electronic Structure of Actinyls: Orbital Properties

Paul S. Bagus,* Connie J. Nelin, Kevin M. Rosso, Bianca Schacherl, and Tonya Vitova

ABSTRACT: A detailed analysis is presented for the covalent character of the orbitals in the actinyls: UO_2^{2+}, NpO_2^{2+}, and PuO_2^{2+}. Both the initial, or ground state, GS, configuration and the excited configurations where a 3d electron is excited into the open valence, nominally the 5f shell, are considered. The orbitals are determined as fully relativistic, four component Dirac-Coulomb Hartree−Fock solutions. Several measures, which go beyond the commonly used population analyses, are used to characterize the covalent character of an orbital in order to obtain reliable estimates of the covalency. Although there are differences in the covalent character of the orbitals for the initial and excited configurations of the different actinyls, there is a surprising similarity in the covalent character for all of the states considered. This is true both between the initial and excited configurations as well as between the different actinyls. The analysis emphasizes the 5f covalent character in the closed shell bonding orbitals and the open shell antibonding orbitals since the focus is on characterizing orbitals needed in a many-body treatment of the actinyl wave functions. However, estimates are also made of the participation of the actinide 6d in the covalent bonding.

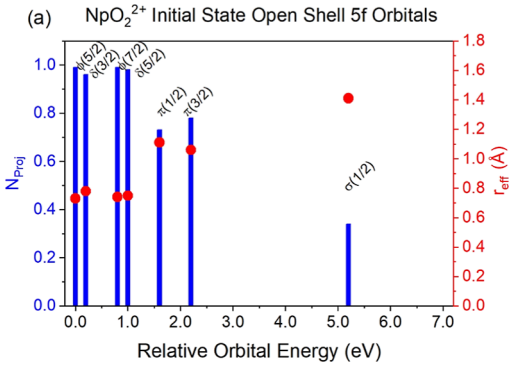

1. INTRODUCTION

The actinide elements have complex and still poorly understood chemical and physical properties. However, their importance remains in topics with significant societal relevance like nuclear medicine, remediation of contaminated sites, short- and long-term safety of nuclear waste disposal, and development of new nuclear fuels for energy generation. X-ray absorption spectroscopies are widely used to characterize the local coordination and speciation of the actinides in these various chemical contexts.[1] In recent years, advances in core-level spectroscopies gain importance for the investigation of electronic structure and bonding phenomena such as covalency.[2,3] Understanding of spectral data from cutting-edge X-ray spectroscopic tools using advanced theory is essential for properly interpreting bonding properties including stability and reactivity relations.[4] However, precise computations remain challenging due to the large number of electrons and their relativistic nature in large actinide systems. One specific open question is, can we infer bond covalency for the actinyl molecules by advanced X-ray spectroscopy and correlate the results to advanced theory?

This paper presents an analysis of the covalent character of the orbitals in the series of actinyls UO_2^{2+}, NpO_2^{2+}, and PuO_2^{2+}. The motivation is to lay the foundation to answering the question of whether core-level spectroscopies, perhaps coupled with detailed theoretical studies, can provide information about the covalent properties of the bonding in the actinyls. The covalency will be examined for the initial state configuration where the core-levels are filled as well as for configurations where a 3d electron is excited to the empty 5f (UO_2^{2+}) or partly occupied 5f (NpO_2^{2+} or PuO_2^{2+}). For the excited configurations, both cases of $M_4 \rightarrow 5f$, where a $3d_{3/2}$ electron is excited to the 5f shell, and $M_5 \rightarrow 5f$, where a $3d_{5/2}$ electron is excited, are examined. This is largely to confirm that the differences between the orbitals optimized for excitation of a $3d_{3/2}$ electron are very similar to those optimized for excitation of a $3d_{5/2}$ electron. There have been several previous theoretical studies of the electronic structure of actinyls, including the covalent character of the actinide cation interaction with the oxygen; see, for example, refs 5−8. However, this study is unique in several respects. First, it examines with a consistent set of measures the covalent character in the full series of actinyls rather than in a single molecule. Second, we used a series of different theoretical measures to obtain assignments of the covalency that are supported by all of these measures. This is an extension of the approach we have taken earlier to characterize the covalent character of plutonium dioxide.[9] Third, we distinguish the covalency, as assigned from the different measures, for the initial and excited configurations. Finally, we distinguish the covalent character of the open shell orbitals in the open valence 5f shell, which are either nonbonding or antibonding, from the character of the closed shell orbitals, which may have

a bonding character. This different bonding character of the closed and open shell orbitals is a standard feature of ligand field theory; see, for example, refs 10,11. We will also examine the extent of the 6d covalency in the closed shell orbitals of gerade (g) symmetry to determine if the involvement of the 6d bonding covalency is different for the various cases. With the foundation laid for the orbital character, we will in a future paper apply this analysis of the orbital covalency as a basis to determine the orbitals to be used in a study of the many-body wave functions of the initial and, especially the M_4 and M_5 excited states. This later work will allow us to obtain theoretical predictions to compare with observed X-ray absorption spectroscopy, XAS, especially for the near-edge XAS, X-ray absorption near edge spectra (XANES).[4,12] However orbital analysis, especially the covalent character of the orbitals, is of value in itself to understand chemical bonds and chemical bonding. This value of orbitals was recognized by Mulliken and he developed the method of population analysis as a means to understand orbital character.[13−16] As well as characterizing the atomistic composition of orbitals, population analysis makes it possible to distinguish bonding from antibonding orbital character. However, it is known that population analysis can sometimes give misleading results,[17,18] and hence, in the present work, we use other methods, rather than population analysis, to determine orbital character.

The description of the chemical bonds in actinyls and the role that is played by bonding and antibonding orbitals is described in detail in the pioneering work of Denning.[19] This included the role that covalent mixing to form fully occupied bonding orbitals as well as unoccupied or partially occupied antibonding orbitals. There is consensus that the covalent mixing of the actinide cation and O ligand anion orbitals plays a key role in the chemistry of the actinyls; see, for example, refs 5−8. In this work, following common practice, we use the mixing[18] of actinide and ligand orbitals as the definition of covalency. This definition is explicitly shown in eq 1 of ref 8 with the parameter λ which governs the mixing of $\phi_M + \lambda\phi_L$, where ϕ_M is an actinyl orbital and ϕ_L is an oxygen orbital. The difficulty is to determine λ, the extent of the covalent mixing of the actinide and oxygen orbitals. The Mulliken population analysis[13−16] does give a decomposition of actinide and ligand character but it is known that there is the possibility of misleading assignments; see, for example refs 18,20. Methods developed by Bader[21] where the space is divided into regions to be associated with either the actinide or the ligand have been used[8] to describe the covalent character of UO_2^{2+} and NpO_2^{2+}. The properties of natural bond orbitals developed by Weinhold and Reed[22,23] have been used[5,6] to describe the covalent character of UO_2^{2+}, NpO_2^{2+}, and PuO_2^{2+}; however, these methods may have limitations as discussed in ref 20. Therefore, we have chosen to use novel theoretical methods and criteria that go beyond the methods used in these previous studies[5−8] of covalency in actinyls. While these newer methods have been used in previous studies of the covalency in heavy metal compounds,[9,20] we briefly review the use of these methods in the present paper.

One of the complexities in the electronic structure of actinyls and of actinide compounds in general arises from the open shell character of the initial and the core-level excited states of the system as well as from the near degeneracies of many of the molecular orbitals which result from the combination of spin−orbit and ligand field splittings, in particular, of the valence orbitals. It should be stressed that a general result from ligand field theory is that the covalent character of the closed shell orbitals is bonding, while the covalent character of valence open shell orbitals, 5f for the actinides, is antibonding; see, for example, Chapter 7 of ref 10. It will be shown that the combination of spin−orbit and ligand field splittings leads to a large number of near degeneracies in the energies of the spin−orbit and ligand field split orbitals. It is to be expected that the near degeneracies of the orbital energies will lead to many-electron WFs that also have nearly degenerate total N electron energies, and these N-electron degeneracies will have consequences for spectroscopies like X-ray photoelectron spectroscopy, XPS, or XAS. Only once we have established the character of the orbitals and the extent of their covalent character will it be possible to define the many-body spaces that must be included in the total wave functions, WFs, of the actinides to give a proper description, especially of the core-excited states. This, then, is a further reason to have a well-founded description of the orbital character and how that character may change for different configurations, both initial and core-excited or ionized configurations. The theoretical requirements these orbital properties impose on the treatment and design of the N electron WFs for the initial and core-excited actinyl configurations will be addressed in a later paper. Indeed, it will be shown there that our choice of orbital spaces to describe the N-electron WFs based on their covalent character leads to satisfactory theoretical predictions of the $M_{4,5}$ near edge XAS of actinyls.

The organization of the article is as follows: In the following section, Section 2 Theoretical Considerations, we describe briefly the methods that we have used to determine orbitals, within a Dirac Hartree−Fock, DHF, framework.[24] We also review the methods used to determine the extent of their covalency and the notations that are needed to characterize these orbitals. The focus of the theoretical descriptions in this section is to emphasize the physical content of the different methods rather than the mathematical content. This is followed in Section 3, Results and Discussion of the Covalent Character of the Molecular Orbitals, by a discussion of the character of the initial and core-excited orbitals. Here, we consider both the open and closed shell orbitals that are used in the many-body treatments. In this section, we also briefly compare our present analysis of the covalency of actinyls with the analyses and assignments in the previous work of refs 5−8. Finally, in Section 4, our conclusions about the bonding are summarized.

2. THEORETICAL CONSIDERATIONS

The configurations and symmetry properties of the initial and excited states of the linear actinyls are considered first. The excitations that are considered are from the $3d_{5/2}$ shell into the 5f shell, denoted M_5 XAS, and from the $3d_{3/2}$ shell into the 5f shell, denoted M_4 XAS. The 3d spin−orbit splitting is large and the M_4 excitation energies are more than 500 eV larger than the M_5 excitation energies. The 5f shell orbitals are both spin−orbit and ligand field split into 5 $f\sigma_{1/2}$, 5 $f\pi_{1/2}$, 5 $f\pi_{3/2}$, $5f\delta_{3/2}$, $5f\delta_{5/2}$, $5f\phi_{5/2}$, and $5f\phi_{7/2}$ sub shells, where the ϕ and δ orbitals are nonbonding and the π and σ orbitals are antibonding.[5,19,25] The subscript for λ_j, where j, which may be either $\lambda - 1/2$ or $\lambda + 1/2$, represents the spin−orbit splitting of λ and the magnitudes of the spin−orbit splittings of the 5f orbitals are $\leq$1 eV. Details of the orbital properties are considered for each actinyl in Section 3.

The orbitals are four component orbitals determined as self-consistent field, SCF, solutions of DHF equations[24] and were optimized separately for the initial and the 3d excited configurations. These orbitals can be used to form determinants which are involved in the calculation of WFs; see, for example, ref 26. For the initial state, the SCF-DHF orbitals are optimized for the configuration

$$3d_{3/2}{}^{4}3d_{5/2}{}^{6}\cdots\cdots 5f^{n} \quad (1)$$

where the average coupling of the n open shell electrons in the 5f shell, distributed in all possible ways over the 14 ligand field and spin−orbit split orbitals, is used.[27] The $UO_2{}^{2+}$ is closed shell and, thus, the n in eq 1 is $n = 0$. The $NpO_2{}^{2+}$ configuration has one electron in an open shell with $n = 1$ in eq 1. For this configuration, there are 14 states distributed over seven different multiplets, which are collections of states with different energies. The $PuO_2{}^{2+}$ configuration has two electrons in the open shell with $n = 2$ in eq 1. For this configuration, there are 91 states distributed over 52 multiplets. The closed $3d_{3/2}$ and $3d_{5/2}$ subshells are explicitly shown in eq 1 since for the excited configurations an electron is removed from one of these subshells. For these excited states, the following configurations are used to obtain the SCF-DHF orbitals

$$3d_{3/2}{}^{3}3d_{5/2}{}^{6}\cdots\cdots 5f^{n+1} \text{ and} \quad (2a)$$

$$3d_{3/2}{}^{4}3d_{5/2}{}^{5}\cdots\cdots 5f^{n+1} \quad (2b)$$

where eq 2a, 2b are for M_4 and M_5 excitations, respectively. These orbitals provide direct information about the covalent character of the actinide−oxygen interaction; furthermore, as we will show in a later paper, they are also appropriate to be used for fully relativistic many-electron WFs; see, for example, ref 9. We note that the SCF-DHF orbitals are for the average of the occupations of the different open shell orbitals[27] of eqs 1 and 2.

In particular, the different sets of orbitals for the initial and excited configurations provide direct information relating the covalency in the excited state to the screening of the open core−shell in the excited configuration. This is because the optimized orbitals for the excited states of eq 2 take account of the response of the valence electrons to the presence of a hole in the core 3d shell of the actinyls.[28] In an equivalent core model, one views the valence electrons, when there is a hole in a core−shell, as moving the field of a nucleus with a charge one greater; i.e., a $Z + 1$ model. Although there are limitations to this $Z + 1$ model,[29] it does clearly show that there may be a major difference in the orbitals that include the physical response to the core-hole. In particular, the use of separately optimized orbitals for each configuration allows us to treat the response in a natural way as an orbital relaxation.[28,30] The differences in the orbital properties for different configurations and for different actinides are examined in the following section. In a future paper, we will present results for the many-body, CI WFs and for the application of these WFs to determine the M_4 and M_5 XANES.

For all the linear actinyls, $AcO_2{}^{2+}$, we used the same bond distance of An−O = 1.77 Å to allow a direct comparison of the properties of the different compounds. This distance is close to values known for actinyls in complexes as reported in ref 12: 1.76 or 1.78 Å for $UO_2{}^{2+}$, 1.75 Å for $NpO_2{}^{2+}$, and 1.74 Å for $PuO_2{}^{2+}$. For the small differences between the nominal An−O distance of 1.77 Å that we have used and the bond distances proposed by Vitova et al.,[12] large changes in the covalent properties of the orbitals are not expected. This has been tested for the case of $PuO_2{}^{2+}$ by comparing the covalent character of the orbitals for the two distances of Pu−O = 1.77 and 1.74 Å. From this comparison, given in the Supporting Information, it is clear that the orbital covalent character is remarkably similar for the two distances. The orbital calculations were performed with a slightly modified version of the relativistic DIRAC program system.[24,31] The Dirac-Coulomb Hamiltonian is used for the orbital calculations. The DIRAC program provides the data for the projection of the orbitals and for the expectation values of orbital properties. Details of the parameters used in the calculation, including basis set exponents, are given in the Supporting Information.

3. RESULTS AND DISCUSSION OF THE COVALENT CHARACTER OF THE INTERACTION OF THE ACTINYLS

3.1. Overview. In this section, we describe the character of the ground and excited state orbitals, as obtained from relativistic DHF solutions for the configurations of eqs 1 and 2, with a focus on their covalent character. In addition to the DHF orbitals for the actinyls, $AnO_2{}^{2+}$, we also determine the DHF orbitals of the isolated +6 actinide cations which are also described by the configurations and open shell occupations of eqs 1 and 2. The comparison of the orbitals of the actinyls and the isolated cations provides a firm basis to access the extent of the covalent interactions.

We begin with a brief comment on the spin−orbit and ligand field split symmetries of these orbitals. For the isolated atoms, there are six degenerate $5f_{5/2}$ orbitals with (j,m_j) values of (5/2, ±5/2), (5/2, ±3/2), and (5/2, ±1/2); the (j,m_j) values for the eight degenerate $5f_{7/2}$ are (7/2, ±7/2), (7/2, ±5/2), (7/2, ±3/2), and (7/2, ±1/2). The axis used for the m_j values is the molecular axis of the linear actinyls, and it is taken as the z axis. Neglecting spin−orbit splitting, the 5f orbitals in the actinyls are split into different values of λ, where λ is the value of l_z for the 5f orbital. This leads to four groups: $5f\phi$, $5f\delta$, $5f\pi$, and $5f\sigma$, where the ungerade notation is not explicitly given because the $D_{\infty h}$ 5f orbitals must be ungerade. When spin−orbit splitting is taken into account, there is additional splitting with $5f\phi$ split into $5f\phi(5/2)$ and $5f\phi(7/2)$ where the quantity in parenthesis is the total symmetry of the orbital, $\omega = \lambda \pm 1/2$; see, for example, ref 32. There are analogous splittings for the other λ values and these orbitals are 2-fold degenerate with m values of $\pm\ \omega$. The good quantum number for the actinyl orbital is ω and components with different λ but the same ω can and do mix. However, in general, this mixing is small and the $5f\lambda(\omega)$ designations remain a useful description; an important concern in this section is to examine the extent to which the open shell orbitals retain their $5f\lambda(\omega)$ character. One way that we measure this is to examine, for the actinyl orbitals, the expectation values of orbital and spin angular momenta, $\langle l_z\rangle$ and $\langle s_z\rangle$, where $j_z = \langle l_z\rangle + \langle s_z\rangle$ must equal $\pm\ \omega$. The significance of these expectation values is the extent of their difference from those for the spin−orbitals of the isolated cations. The difference of the valence orbitals of an actinyl from those of the isolated actinide cation are also shown by the spin−orbit splittings of the different λ components. In addition, there are three properties that provide detailed information about the covalent character of the open shell valence, 5f, orbitals; these properties have been used in earlier studies of PuO_2[9] and of transition metal oxides.[33,34] The first

property concerns the orbital energies of the different 5f orbitals; specifically, the relative orbital energies, $\Delta\varepsilon$, where $\Delta\varepsilon = 0$ for the lowest energy nonbonding 5f orbital and increases in $\Delta\varepsilon$ for the other orbitals can be related to the extent of their antibonding character. This is because orbitals with greater covalent character will be less strongly bound and will have larger values of $\Delta\varepsilon$. The second property, which is a measure of covalent character, is the size of the orbital since a larger contribution of O(2p) character in the nominally 5f orbital will lead to greater size. This orbital size or extent can be quantified with $r_{eff} = [\langle r^2\rangle]^{1/2}$, where r is the radial distance from the actinide center at $r = 0$. The values of $\langle r^2\rangle$, the standard quantum mechanical expectation value of r^2,[26,35] are examined for both open and closed shell orbitals and provide a direct measure of their covalent character since they can be directly compared to the $r_{eff} = [\langle r^2\rangle]^{1/2}$ for the isolated cations given in the Supporting Information. To place the values of r_{eff} in context, we note that the r_{eff} of the actinide 5f orbitals are ~0.7 Å compared to a contracted orbital centered on an O center which would have r_{eff} = 1.77 Å. Thus, r_{eff} for the actinyl orbitals provides a measure of the extent of mixing of O(2p) character with the actinide 5f character. A third measure of covalent character is the projection, N_{proj}, of the $5f_{5/2}$ and $5f_{7/2}$ orbitals of the isolated 6+ cation on the orbitals of the actinyl. The $5f_{5/2}$ orbital projection on a particular actinyl orbital is defined as the sum of the projections of the three degenerate atomic $5f_{5/2}$ orbitals and the $5f_{7/2}$ orbital projection involves the sum of projections for the four degenerate atomic $5f_{7/2}$ orbitals; details of the projections are given in ref 9. If the actinyl orbital is an ideal or pure 5f orbital of the isolated cation, $N_{proj} = 1$, and if the actinyl orbital has no 5f character, $N_{proj} = 0$. We also examine the bonding covalent character of the actinide 6d in the closed shell orbitals of gerade symmetry. For this purpose, we consider as a measure of covalency only the projection of the 6d orbital of the actinide 6+ cation on the gerade actinyl orbitals. While the projection of the more diffuse 6d orbitals may provide an overestimate of the participation of the 6d in the covalent bonding,[20] it will show whether there are significant differences in the covalent participation of the 6d for the different configurations and the different actinyls. For the participation of 6d, the only concern is for the sum of the projections over the occupied closed shell orbitals. Further details about these three measures of covalency are given in ref 9. The effective sizes, spin−orbit splittings, and angular momenta, $\langle l_z\rangle$ and $\langle s_z\rangle$, of the orbitals of the isolated Ac^{6+} cations are given in the Supporting Information and are compared, in the discussion below, with the nominally 5f open shell orbitals of the actinyls.

It is noted that for the orbital projections, we have used the orbitals of the isolated actinide +6 cation. Of course, because of the covalent mixing of actinide 6d and 5f orbitals with O orbitals, the true effective charge of the actinide cation in the actinyl is expected to be considerably smaller than the nominal oxidation state of +6. Thus, one could be concerned that the projected values might be significantly different if a different charge state of the actinide cation had been used to determine the atomic 5f and 6d orbitals for the projection. We do not expect this to be a concern with regard to our use of the projections to measure covalency for the following reasons. The 5f and 6d orbitals for different charge states of the actinide cations have a similar character, albeit somewhat more diffuse or somewhat more contracted, for charge states of the actinide cations between +6 and +2. For the representative case of U, the overlaps of the 5f and 6d orbitals between those optimized for U^{6+} and for the $5f^16d^1$ configuration of U^{4+}, where U^{4+} may be closer to the effective U charge expected for UO_2^{2+}, are almost 1. Specifically, the overlaps of the U^{6+} $5f_j$ with U^{4+} $5f_j$ orbitals are 0.9999 for both $j = 5/2$ and $j = 7/2$ and the overlaps of the U^{6+} and U^{4+} 6d orbitals are 0.996 (3/2) and 0.995(5/2). Clearly, these overlaps are very close to 1 and the atomic 5f and 6d projections on the UO_2^{2+} will be essentially identical whether the atomic orbitals for the U^{6+} or U^{4+} cation are used. Even for the extreme case where the 5f and 6d orbitals are optimized for the.....$5f^36d^1$ configuration of U^{2+}, the overlaps of the U^{2+} orbitals with the U^{6+} are still large; 0.99 for the 5f orbitals and 0.93 for the 6d. Furthermore, since the concern is for trends rather than absolute values of the projections, the changes in the projections using different cation atomic orbitals becomes less important. There is a closely related concern that we will use the atomic orbitals for the initial state configuration of eq 1 to project on the actinyl orbitals for both the initial and excited configurations. It could be argued that the atomic orbitals for the excited configuration of eq 2 should be used to determine the 5f and 6d orbital occupations for the orbitals optimized for the actinyl excited configuration. However, here also, the 5f and 6d atomic orbitals are very similar whether they have been optimized for eqs 1 or 2. The overlap of the U 5f and 6d orbitals for the initial and excited configurations is extremely close to 1. Specifically, the overlap of the 5f orbitals for the initial configuration and for the $M_5 \rightarrow$ 5f configuration is 0.992 and the overlap of the 6d orbitals is 0.9995. These overlaps are sufficiently close to 1, that the initial configuration 5f and 6d orbitals can be used to project the character of both the initial and excited configuration actinyl orbitals; the equivalent overlaps for the $M_4 \rightarrow$ 5f orbitals are essentially identical to those for the $M_5 \rightarrow$ 5f orbitals. It is clear that similar results, as described for U, will also hold for the Np and Pu atomic orbitals. They fully justify our use of the orbitals optimized for the +6 cation initial configuration, eq 1, to determine, in the following subsections, the projections of the 5f and 6d character of the actinyls.

3.2. Bonding Analyses of the Valence Orbitals of NpO_2^{2+}. We begin an analysis of the relevant orbitals of the actinyls with a discussion of the initial state orbitals of NpO_2^{2+}; we choose to begin our analysis of the neptunyl orbitals because the 5f open shell is occupied in the initial, or ground state (GS), configuration with one electron, see eq 1, and we can directly compare the occupied 5f orbitals in the initial, eq 1, and the 3d excited configurations, eq 2. The comparison is somewhat more complicated for UO_2^{2+} since the GS of UO_2^{2+} is a closed shell and the nominally U 5f orbitals are not occupied. Thus, we discuss the properties of the actinyl orbitals in the sequence NpO_2^{2+}, PuO_2^{2+}, and UO_2^{2+}.

The properties of the NpO_2^{2+} initial configuration orbitals are shown in Figure 1. The orbitals specifically considered are the open shell, nominally 5f, orbitals which have an occupation of 1 electron, Figure 1a and the three closed shell orbitals that have a significant amount of 5f character, Figure 1b. The three closed shell orbitals were selected because they contain almost 95% of the total 5f character, as given by projection, in the closed shells. Thus, these are orbitals that should be included in the active space of CI calculations of the many electron WFs. Detailed information about the orbital properties including projections and angular momentum expectation values is given in Table SIII of the Supporting Information. For

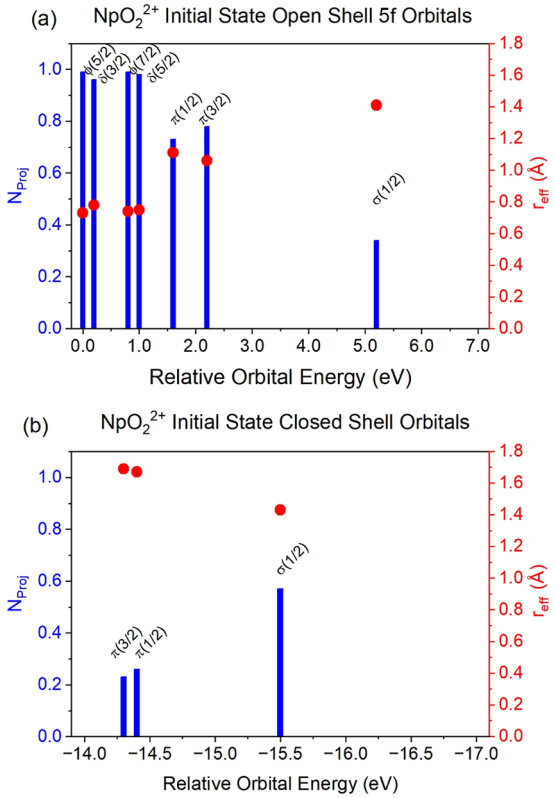

Figure 1. Properties of key orbitals for the initial configuration of NpO_2^{2+}: (a) seven open shell orbitals and (b) three closed shell orbitals. The N_{proj} are vertical bars with scale on left; the r_{eff} are filled circles; and the orbital characters are shown as $\lambda(\omega)$ for each orbital; see text.

the initial state configuration for which these orbitals were optimized, eq 1, the seven open shell orbitals have an average occupation of 1/7 and the closed shell orbitals have an occupation of 2 electrons. Three properties are shown for each orbital. The vertical blue bar is the projection, N_{proj}, of the Np^{6+}(5f) orbitals on the NpO_2^{2+} orbitals with the range for projection, $0 \le N_{proj} \le 1$, shown on the left. The red circles are measures of the "effective" orbital sizes given as r_{eff}, as defined above. Finally, the dominant character of the orbital is shown by $\lambda(\omega)$ above each orbital where the effective value for λ is obtained from the $\langle l_z \rangle$ given in the Supporting Information. For each orbital, these three properties are centered above the relative orbital energy, $\Delta\varepsilon$ in eV, of the orbital with $\Delta\varepsilon = 0$ for the lowest energy 5fϕ(5/2) orbital. As measures of the covalency in the closed shells, we also give in Table 1, the 5f and 6d occupations in these closed shells. The occupations are simply the sum of the 2* N_{proj} (5f) and 2*N_{proj}(6d) over all the closed shell orbitals, where the factor of 2 simply represents the total occupation of that orbital. In Table 1, the closed shell occupations for UO_2^{2+} and PuO_2^{2+} are also given to facilitate

Table 1. Occupations of Actinide 5f, Occ(5f), and 6d, Occ(6d), in the Closed Shells of the Initial State Configuration of the Different Actinyls as Obtained from Projections

	UO_2^{2+}	NpO_2^{2+}	PuO_2^{2+}
Occ(5f)	2.32	2.25	2.42
Occ(6d)	2.71	2.67	2.61

the comparison of these actinyls, as discussed later. It is clear from Table 1 that there is a large 6d occupation of 2.67 electrons, which suggests a significant contribution of the Np(6d) to the covalent bonding.

In Figure 1a, the third open shell orbital of NpO_2^{2+} has $\Delta\varepsilon$ = 0.80 eV and ω = 7/2; it is a pure Np($5f_{7/2}$) orbital belonging to the linear symmetry ϕ as is clearly shown by the projections and other properties in Table SIII. Clearly, this orbital is nonbonding. For this nonbonding ϕ orbital, the projection of the Np $5f_{7/2}$ orbital is $N_{proj}(5f_{7/2})$ = 0.99 not 1.0 and the r_{eff} = 0.74 is larger than the value of r_{eff} = 0.67 for the $5f_{7/2}$ orbital of isolated Np^{6+}, see the Supporting Information. The reason for these deviations is that Np cation in NpO_2^{2+} has an effective charge which is much smaller than the nominal +6 for Np(VI) because there is considerable covalent character in the open shells, see Figure 1a, and in the closed shells, see Figure 1b and Table 1.

Deviations from ideal values of the projections and r_{eff} will also be seen for the other nonbonding Np(5f) orbitals and are discussed in the Supporting Information. The significant conclusion is that properties of these orbitals depart slightly from the values for the isolated cation, Table SI, because the effective ionicity is significantly smaller than the nominal +6. A similar analysis assigns orbitals 2 and 4 in Figure 1a as being dominantly the spin−orbit split 5fδ(3/2) and 5fδ(5/2); see the discussion in the Supporting Information. The splitting of the δ orbitals from their ϕ counterparts is small, ~0.2 eV, and this small splitting is consistent with their being nonbonding. The r_{eff} values for these 5fδ orbitals are close to those for the 5fϕ orbitals and this also shows that they are nonbonding. In particular, the values of r_{eff} for the antibonding π and σ orbitals, 5−7 in Figure 1a, are significantly larger. The values of $\langle l_z \rangle$, shown in Table SIII, provide a useful way to assign the value of λ for the orbitals. The π character of orbitals 5 and 6 in Figure 1, described as 5fπ(1/2) and 5fπ(3/2), is shown by the $\langle l_z \rangle$ = 0.95 and 1.07 for these orbitals. Their antibonding covalent character is shown by the values of $\Delta\varepsilon$ which are ~1.5 eV larger than the $\Delta\varepsilon$ for the nonbonding 5fϕ and 5fδ orbitals. Their larger values of $r_{eff} \approx$ 1.1 Å, ~35% larger than for the nonbonding orbitals, indicates that there is a significant amount of O character, primarily, O(2p), in these orbitals. The values of the total 5f projection, N_{proj}(5f), for these 5fπ orbitals would suggest that they have 25% O character. This covalent mixing with O(2p) is consistent with an ~25% reduction in the spin−orbit splitting of these orbitals from the values for the ϕ and δ orbitals; see Table SIII. Also, for the 5fπ(1/2) orbital, there is a strong mixing of $5f_{5/2}$ and $5f_{7/2}$ character as shown by the projections of $5f_{5/2}$ and $5f_{7/2}$ in Table SIII. The seventh open shell orbital has $\langle l_z \rangle$ = 0.08 and is described as 5fσ(1/2). It has much larger antibonding character with the largest $\Delta\varepsilon$ = 5.25 eV. Its r_{eff} = 1.42 Å, which approaches the Np−O distance of 1.77 Å is consistent with an orbital where the 5f projection, N_{proj}(5f) = 0.34, indicates that it has only 35% Np character.

The projections for the three closed shells in Figure 1b and Table SIII show that they have between 25 and 60% N_p 5f character. Their orbital energies, $\Delta\varepsilon \approx -15$ eV, show that they have significant bonding character between Np(5f) and O(2p). Indeed, the data in Table SIII show that they account for almost 95% of the covalent bonding Np(5f) character in the closed shells, which sums to an occupation of over 2 Np(5f) electrons. This is a major change from the nominal assignment of no 5f character for the closed shell orbitals. The analysis of

the excited state orbitals will show a similar large bonding character for the closed shell orbitals. The bonding character of these closed shell orbitals is a clear indication that they should be included in the active space for determining N electron many-body WFs for the actinyls.[5,7] Thus, it is important to understand how the bonding character of these orbitals may be different for the excited state configuration and for other actinyls.

The properties for the orbitals optimized for the $M_5 \rightarrow 5f$ excitation and for the $M_4 \rightarrow 5f$ excitation are reasonably similar to those for the initial state of NpO_2^{2+} which were shown in Figure 1 and Table SIII. The same open and closed shell properties that were given in Figure 1 for the initial state configuration are given in Figure 2 for the orbitals of the $M_5 \rightarrow$

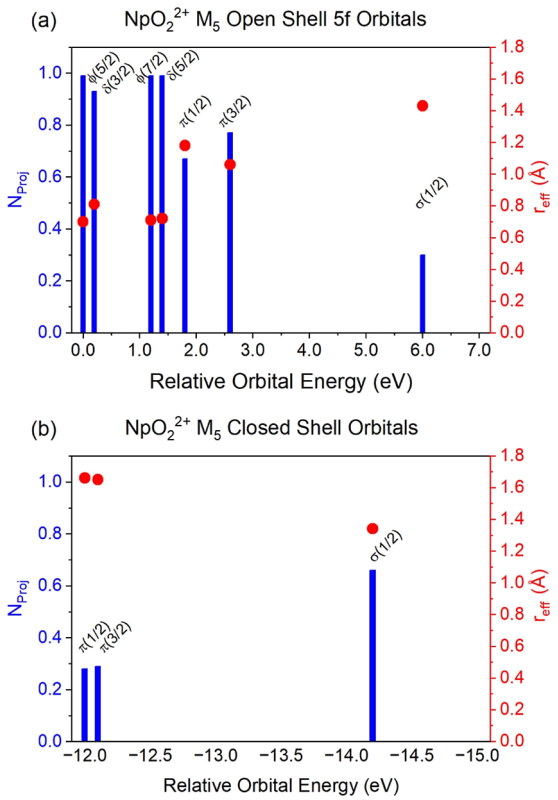

Figure 2. Properties of key orbitals for the $M_5 \rightarrow 5f$ configuration of NpO_2^{2+} with (a) open shell and (b) closed shell orbitals; see the caption to Figure 1 and text.

5f excited configuration. Comparable details as in Table SIII are given in Table SIV for the $M_5 \rightarrow 5f$ and Table SV for the $M_4 \rightarrow 5f$ excited configuration orbitals. Because the properties of these orbitals are so similar for the $M_5 \rightarrow 5f$ and $M_4 \rightarrow 5f$ excited configurations, a figure showing orbital properties is not given for the $M_4 \rightarrow 5f$ excited orbitals; however, see Table SV for these orbital properties. A significant difference between the initial and $M_5 \rightarrow 5f$ excited state orbitals concerns the changes in the covalent bonding character in the closed shells, as shown in Table 2 for the 5f and 6d occupations of the excited configuration; the format of this table parallels Table 1. To facilitate the comparison of the 5f and 6d closed shell occupations for the initial and the $M_5 \rightarrow 5f$ configurations, the data from Tables 1 and 2 is shown graphically in Figure 3 where the occupations are shown in bars which are gray for the 5f and blue for the 6d occupations.

Table 2. Occupations of Actinide 5f, Occ(5f), and 6d, Occ(6d), in the Closed Shells of the Excited $M_5 \rightarrow 5f$ configuration of the Different Actinyls as Obtained From Projections

	UO_2^{2+}	NpO_2^{2+}	PuO_2^{2+}
Occ(5f)	2.63	2.61	2.84
Occ(6d)	2.70	2.64	2.58

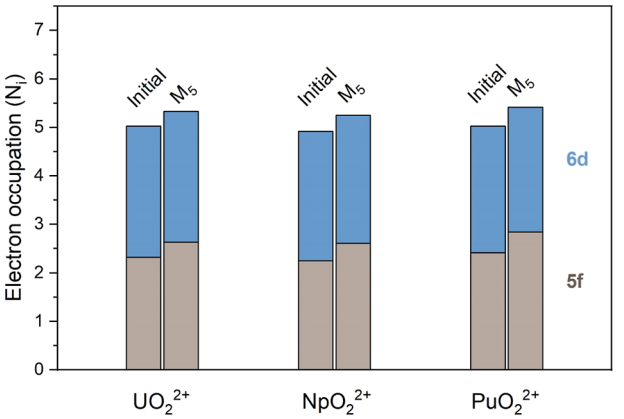

Figure 3. Closed shell occupations, from the data in Tables 1 and 2, of Actinide 5f (gray bars) and 6d (blue bars) for the initial and M_5 ($M_5 \rightarrow 5f$) configurations for UO_2^{2+}, NpO_2^{2+}, and PuO_2^{2+}.

There is a modestly larger covalent 5f bonding character in the closed shell orbitals of the excited configuration. The 5f occupation in the closed shells for the $M_5 \rightarrow 5f$ increases by about 15% from the GS occupation, while the 6d occupation is very similar to that for the GS. The modest changes in the 5f occupation arise because the O electrons see a somewhat larger effective charge from the Np cation due to the excitation from a contracted 3d orbital to a more extended 5f orbital. Other significant differences between the initial configuration orbitals and the $M_5 \rightarrow 5f$ excited configuration orbitals are (1) the larger effective charge of the Np cation also leads to the 5fπ and 5fσ orbitals of the excited configurations having slightly greater antibonding character than for the initial configuration, see Figure 1a and 2a. The increase in antibonding character is shown by the changes, increases, in the relative valence, 5f, open shell orbital energies, $\Delta\varepsilon$, as shown in Figures 1a and 2a and Tables SIII, SIV, and SV. The increase is most important for the 5fσ(1/2) orbital which has an increase in $\Delta\varepsilon$, of 0.5 eV for $M_4 \rightarrow 5f$ and 0.8 eV for $M_5 \rightarrow 5f$; these are increases of between 10 and 15%. (2) The gap between the orbital energies of the lowest valence open shell orbital and the closed shell orbitals with significant 5f character is lower by ~2.0 eV for the initial configuration compared to the $M_5 \rightarrow 5f$ configuration. There are similar changes in the orbital energy gap between the initial and the $M_4 \rightarrow 5f$ configurations. The origin of this change in the orbital energy gap can be viewed as the greater effective nuclear charge in the valence of Np because the localized Np 3d orbital has been promoted to the diffuse 5f open shell. These minor differences show that the impression given by the orbital properties for the initial configuration, Figure 1 and Table SIII, also holds for the orbitals optimized for the excited configurations. This is an important result in that it shows that the orbitals appropriate for the excited configurations, eq 2, have a covalent character that is rather similar to that for the orbitals appropriate for the initial state.

We close this subsection by noting that our analysis of the orbital covalency for the initial and excited configurations of NpO_2^{2+} has given novel and direct information about the covalent character of these orbitals. The differences and similarities with the other actinyls, PuO_2^{2+} and UO_2^{2+}, will be considered in the following subsections. We postpone a comparison of our assignments of the covalency of the initial and excited configurations of NpO_2^{2+} with previous studies[3,6] to a later subsection, Section 3.5, where we will consider comparisons for all three actinyls.

3.3. Bonding Analyses of the Valence Orbitals of PuO_2^{2+}. We consider next the properties of the orbitals optimized for the initial configuration of PuO_2^{2+} which are shown in Figure 4 and Table SVI. The format of the data

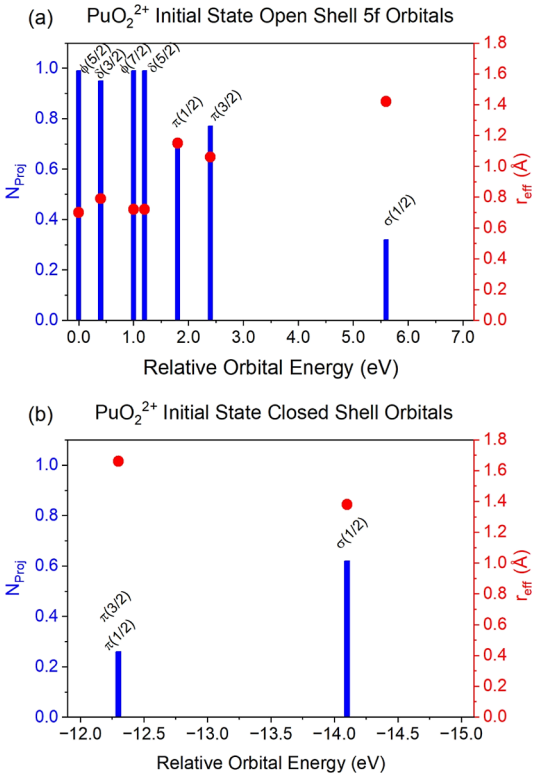

Figure 4. Properties of key orbitals for the initial configuration of PuO_2^{2+}: (a) seven open shell orbitals and (b) three closed shell orbitals; see the caption to Figure 1

shown for PuO_2^{2+} parallels that presented for NpO_2^{2+} and the discussion of the data will be brief. Indeed, the PuO_2^{2+} orbital properties for the initial configuration are quite similar to those discussed above for NpO_2^{2+} with a few minor differences. The $\Delta\varepsilon$ values are slightly larger for PuO_2^{2+} than for NpO_2^{2+} mainly because the spin−orbit splitting of the $5f_{5/2}$ and $5f_{7/2}$ orbital energies is expected to be larger for the Pu cation in PuO_2^{2+} than for the Np cation in NpO_2^{2+}. An estimate of the different spin orbit splitting in the actinyls can be made by comparing the 5f spin−orbit splitting in isolated Pu and Np cations. For example, the 5f orbital energy spin orbit splitting is 0.15 eV larger for Pu^{6+} than for Np^{6+}; see Table SI. The closed shell 5f and 6d occupations for PuO_2^{2+}, see Table 1 and Figure 3, are very similar to those for NpO_2^{2+}. One difference is that the Pu 5f closed shell occupation, 2.42 electrons, is 0.17 electrons greater than the Np 5f closed shell occupation. On the other hand, the Pu(6d) occupation for the initial configuration of PuO_2^{2+} is essentially the same as for NpO_2^{2+}, very slightly, 2%, smaller. The orbital properties for the orbitals optimized for the PuO_2^{2+} $M_5 \rightarrow 5f$ excited configuration are shown in Figure 5 and Table SVII; those for the $M_4 \rightarrow 5f$ configuration are

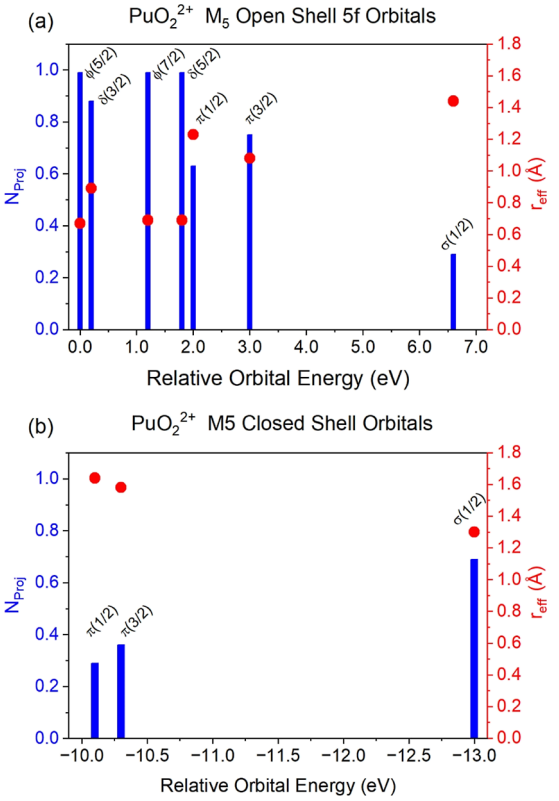

Figure 5. Properties of key orbitals for the $M_5 \rightarrow 5f$ configuration of PuO_2^{2+} with (a) open shell and (b) closed shell orbitals; see the caption to Figure 1

given in Table SVIII. The same comments about the differences between the initial and excited configuration orbitals as those made for NpO_2^{2+} also apply for PuO_2^{2+}. Simply put, the properties of the PuO_2^{2+} orbitals for both the initial and excited configurations are similar to those for the NpO_2^{2+} orbitals for these configurations.

3.4. Bonding Analyses of the Valence Orbitals of UO_2^{2+}. Finally, we examine the 5f and 6d covalencies in UO_2^{2+}. The open shell 5f character for the initial or GS configuration is not rigorously defined for UO_2^{2+} since it is a closed shell configuration that is nominally $5f^0$. Hence, the dominantly 5f orbitals of UO_2^{2+} would have to be taken from the virtual, unoccupied, space; however, these virtual orbitals are more appropriate for U in a formal U(V) oxidation state than in the formal U(VI) oxidation state of UO_2^{2+}.[26,35] We also found that, for the virtual orbitals of the GS configuration, the $5f\sigma$ character was spread over a few virtual orbitals making it difficult to identify a $5f\sigma(1/2)$ for U. On the other hand, the orbitals optimized for the excited state configurations, where the dominantly 5f open shell orbitals are occupied, will give orbitals comparable to those for the excited configurations of the other actinyls. Thus, we present in Figure 6 and Table SIX orbital properties for the $M_5 \rightarrow 5f$ excited configuration of UO_2^{2+} and in Table SX orbital properties for the $M_4 \rightarrow 5f$ configurations; this information is in the same format as used previously. The U 5f and 6d occupations in the closed shells of

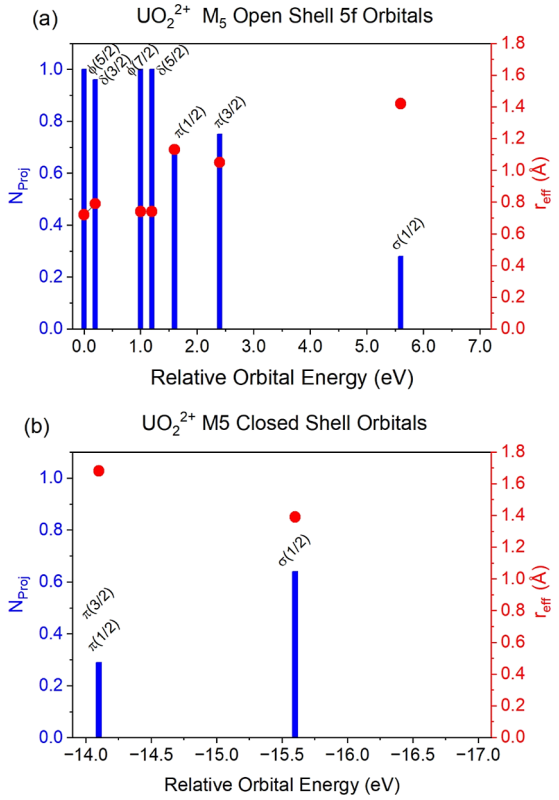

Figure 6. Properties of key orbitals for the $M_5 \rightarrow 5f$ configuration of UO_2^{2+} with (a) open shell and (b) closed shell orbitals; see caption to Figure 1

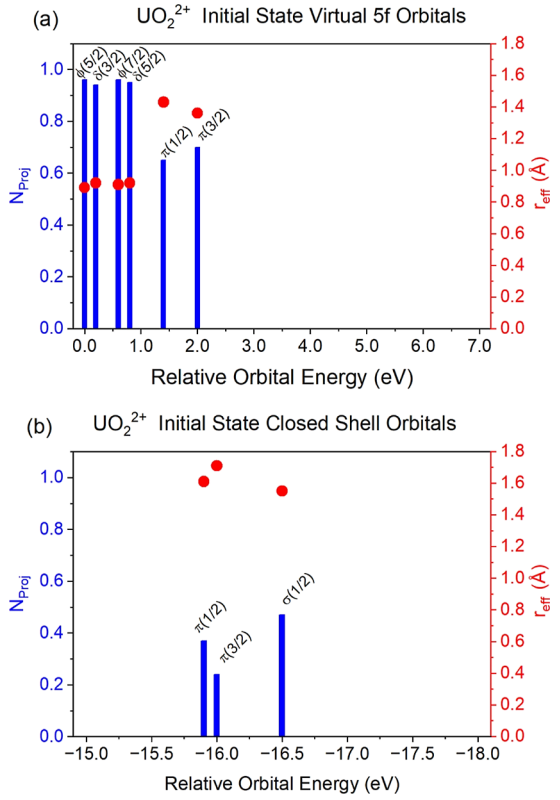

Figure 7. Properties of key orbitals for the initial configuration of UO_2^{2+}: (a) six virtual orbitals and (b) three closed shell orbitals; see the caption to Figure 1. A dominantly U 5fσ(1/2) orbital could not be identified among the virtual orbitals and is not included.

UO_2^{2+} are given in Table 1 (initial configuration) and Table 2 ($M_5 \rightarrow$ 5f excited configuration). The open shell orbital properties for excited configurations of UO_2^{2+} are quite similar to those for the other actinyls; see Figures 2 and 5 and the data in the appropriate Supporting Information tables. The main difference is that the orbital energy splittings are somewhat smaller for UO_2^{2+} than those for NpO_2^{2+} and PuO_2^{2+} because there is a smaller spin−orbit splitting of the U 5f orbitals than that of the Np or Pu 5f orbitals. The three closed shell orbitals with large 5f character have, as for the other actinyls, a very large fraction. ∼95%, of the total covalent bonding 5f occupation. The U 6d occupation in the closed shells, Table 2, is also similar to that of the other actinyls.

For the sake of completeness, we also give, in Figure 7 and Table SXI, the orbital properties for the initial configuration of UO_2^{2+}. As we noted above, for the orbitals analogous to the valence open shells of the other actinyls, it was necessary to use the lowest lying virtual orbitals. For the lower lying "open" shell orbitals, these virtual orbitals were similar to the occupied open shell orbitals of the initial configuration of the other actinyls. However, the 5fσ character was distributed over more than 1 virtual orbital and the seventh virtual "5f" orbital in Table SXI has too little 5f character and it also has a very large r_{eff}; for these reasons, it is not included in Figure 7. Otherwise, the properties of the UO_2^{2+} initial configuration 5f orbitals are similar to those for the other actinyls.

3.5. Comparison with Prior Assignments. We close Section 3 on the orbital covalent character with a brief description of the assignments and assessments of the covalency given in the prior studies of refs 5−8. Gendron et al.[5] describe the electronic character and magnetic properties of NpO_2^{2+}. They clearly state that the covalent character of the orbitals is included in the theoretical methods used to determine the complete active space self-consistent field,[36] CASSCF, WFs used in their study. The covalent character of certain of the CASSCF orbitals is shown in isosurface orbital plots, but no quantitative estimate of the covalency is given. The analysis of Sergentu et al.[6] is also based on CASSCF WFs and uses the properties of natural localized molecular orbitals, NLMOs; it is reported for UO_2^{2+}. NpO_2^{2+}, and PuO_2^{2+}. It is difficult to compare our results with those of Sergentu et al.[6] because of the different approaches that have been taken. We sum over the 5f and 6d projections of the covalency in all the closed shell orbitals to obtain the occupations reported in Tables 1 and 2. On the other hand Sergentu et al.[6] report the composition only for selected NLMOs in their Figures 4 and 5. The total An 5f and 6d occupations from the localized orbitals shown in their figures are considerably smaller than that reported in Tables 1 and 2. This may be because the total 5f and 6d occupations come because there are contributions from other NLMOs besides those shown in their figures. For example, we have shown explicitly that there are three closed shell orbitals that have significant An 5f character and the same could easily be true for the NLMOs used in the Sergentu et al.[6] analysis. The work of Polly et al.[7] on the resonant inelastic X-ray scattering. RIXS of UO_2^{2+} also uses WFs determined with a CASSCF methodology. They explicitly state that the covalent character of the orbitals is an important criterion in the choice of orbitals to be used in the CASSCF active space, and this is quite correct. However, no details are given on the extent of the covalent character of the CASSCF orbitals. The work of

Stanistreet-Welsh and Kerridge[8] is concerned with analyzing how covalency can be extracted from XAS spectra. It uses a variant of the CASSCF methodology to determine WFs so that the covalent character of the orbitals is certainly included in the WF calculations. However, they do not give information on the orbital covalency that can be directly compared to that in our analysis.

4. CONCLUSIONS

We have presented a detailed analysis of the covalent bonding and antibonding character of the orbitals for the initial and excited, $M_5 \rightarrow 5f$ and $M_4 \rightarrow 5f$, configurations of the series of actinyls, UO_2^{2+}, NpO_2^{2+}, and PuO_2^{2+}. This study is unique in several respects: (1) The orbitals were obtained from fully relativistic self-consistent field solutions of Dirac−Fock calculations with the Dirac-Coulomb Hamiltonian. For each configuration, the orbitals were optimized separately for the average of the open shell couplings, described as average of configurations.[27] In particular, separate sets of orbitals were optimized for each of the three initial, $M_5 \rightarrow 5f$, and $M_4 \rightarrow 5f$, configurations. In this way, the relaxation, or response, of the "passive" orbitals to the excitation was taken into account. (2) Several different measures were used to characterize the covalent character, especially for the open shell orbitals. This allowed us to ensure that we have a consistent measure of the covalent character of these orbitals. For the covalent character of the closed shell orbitals, the projection of the orbitals of the isolated cations was used to identify the orbitals with significant 5f character. In addition, we have summed the 5f or 6d projections over all closed shell orbitals. This summation has made it possible to determine the large occupations that the An 5f and 6d would have in total WFs constructed with these orbitals. This explicit examination of the covalency of the full set of orbitals is unique and different from previous studies,[5−8] where the covalent character of all the occupied orbitals has not been reported. This demonstrates that both the 5f and 6d cation orbitals participate in the interaction and chemical bonding of the actinyls.

Although there are differences, the covalent characters of the orbitals for all of the actinides and for both the initial and excited configurations have strong similarities. In all cases, the valence open shell, nominally 5f orbitals, are clearly divided into three groups: nonbonding ϕ and δ orbitals, antibonding π orbitals, and strongly antibonding σ orbitals. Of course, there may be additional ligand field and spin−orbit splittings. For each of the configurations of all of the actinyls, there are three closed shell orbitals with significant 5f character; these three orbitals contain ∼95% of the total projected 5f character in the closed shells. The total closed shell occupations from the projection of the actinyl 5f and 6d orbitals are significant. For the initial configurations, they are greater than 2 and less than 3 electrons, indicating a significant contribution to the bonding from these covalent mixings. For the excited state configurations, the 5f occupations in the closed shells are ∼15% larger than those in the initial configuration, indicating that they can be viewed as playing a role in "screening" the excitation. The 6d occupations for the excited configurations are almost the same as for the initial configuration, only very slightly smaller, indicating that the 6d does not play a role similar to that of the 5f in screening the excitation.

Overall, these results provide insights into the similar character of the bonding for the different actinyls. They also establish a sound chemical basis for the selection of active orbitals for many-body treatments. In particular, this analysis of orbital covalency makes it possible to choose the active spaces for many electron WFs that are used to study the $M_{4,5}$ XAS, which will be reported in a later paper. Indeed, the use of the orbital covalent character to design many-body WFs has been a significant motivation for the orbital analysis made in this paper.

AUTHOR INFORMATION

Corresponding Author

Paul S. Bagus − *Department of Chemistry, University of North Texas, Denton, Texas 76203-5017, United States;* orcid.org/0000-0002-5791-1820; Email: Paul.Bagus@unt.edu

Authors

Connie J. Nelin − *Consultant, Austin, Texas 78730, United States*

Kevin M. Rosso − *Pacific Northwest National Laboratory, Richland, Washington 99352, United States;* orcid.org/0000-0002-8474-7720

Bianca Schacherl − *Karlsruhe Institute of Technology (KIT), Institute for Nuclear Waste Disposal (INE), Karlsruhe D-76021, Germany;* orcid.org/0000-0003-4542-0108

Tonya Vitova − *Karlsruhe Institute of Technology (KIT), Institute for Nuclear Waste Disposal (INE), Karlsruhe D-76021, Germany;* orcid.org/0000-0002-3117-7701

Notes

The authors declare no competing financial interest.

ACKNOWLEDGMENTS

PSB gratefully acknowledges support from the U.S. Department of Energy, Office of Science, Office of Basic Energy Sciences, Chemical Sciences, Geosciences, and Biosciences (CSGB) Division through its Geosciences program at Pacific Northwest National Laboratory (PNNL). PNNL is a multiprogram national laboratory operated for the DOE by Battelle Memorial Institute under contract no. DE-AC05-76RL01830. T.V., B.S., and P.B. acknowledge funding from the European Research Council (ERC) Consolidator grant 2020 under the European Union's Horizon 2020 research and innovation program. (grant agreement no. 101003292).

REFERENCES

(1) Rothe, J.; Altmaier, M.; Dagan, R.; Dardenne, K.; Fellhauer, D.; Gaona, X.; González-Robles Corrales, E.; Herm, M.; Kvashnina, K. O.; Metz, V.; Pidchenko, I.; Schild, D.; Vitova, T.; Geckeis, H. Fifteen Years of Radionuclide Research at the Kit Synchrotron Source in the

Context of the Nuclear Waste Disposal Safety Case. *Geosciences* **2019**, *9*, 91.
(2) Neidig, M. L.; Clark, D. L.; Martin, R. L. Covalency in F-Element Complexes. *Coord. Chem. Rev.* **2013**, *257*, 394−406.
(3) Kaltsoyannis, N. Does Covalency Increase or Decrease across the Actinide Series? Implications for Minor Actinide Partitioning. *Inorg. Chem.* **2013**, *52*, 3407−3413.
(4) Vitova, T.; Faizova, R.; Amaro-Estrada, J. I.; Maron, L.; Pruessmann, T.; Neill, T.; Beck, A.; Schacherl, B.; Tirani, F. F.; Mazzanti, M. The Mechanism of Fe Induced Bond Stability of Uranyl(V). *Chem. Sci.* **2022**, *13*, 11038−11047.
(5) Gendron, F.; Páez-Hernández, D.; Notter, F.-P.; Pritchard, B.; Bolvin, H.; Autschbach, J. Magnetic Properties and Electronic Structure of Neptunyl(Vi) Complexes: Wavefunctions, Orbitals, and Crystal-Field Models. *Cehm.Eur. J.* **2014**, *20*, 7994−8011.
(6) Sergentu, D.-C.; Duignan, T. J.; Autschbach, J. Ab Initio Study of Covalency in the Ground Versus Core-Excited States and X-Ray Absorption Spectra of Actinide Complexes. *J, Phys. Chem. Lett.* **2018**, *9*, 5583−5591.
(7) Polly, R.; Schacherl, B.; Rothe, J.; Vitova, T. Relativistic Multiconfigurational Ab Initio Calculation of Uranyl 3d4f Resonant Inelastic X-Ray Scattering. *Inorg. Chem.* **2021**, *60*, 18764−18776.
(8) Stanistreet-Welsh, K.; Kerridge, A. Bounding [Ano2]2+ (an = U, Np) Covalency by Simulated O K-Edge and an M-Edge X-Ray Absorption near-Edge Spectroscopy. *Phys. Chem. Chem. Phys.* **2023**, *25*, 23753−23760.
(9) Bagus, P. S.; Schacherl, B.; Vitova, T. Computational and Spectroscopic Tools for the Detection of Bond Covalency in Pu(IV) Materials. *Inorg. Chem.* **2021**, *60*, 16090−16102.
(10) Ballhausen, C. J. *Introduction to Ligand Field Theory*; McGraw-Hill: New York, 1962.
(11) Griffith, J. S. *The Theory of Transition-Metal Ions*; Cambridge Press: Cambridge, 1971.
(12) Vitova, T.; Pidchenko, I.; Fellhauer, D.; Bagus, P. S.; Joly, Y.; Pruessmann, T.; Bahl, S.; Gonzalez-Robles, E.; Rothe, J.; Altmaier, M.; Denecke, M. A.; Geckeis, H. The Role of the 5f Valence Orbitals of Early Actinides in Chemical Bonding. *Nat. Commun.* **2017**, *8*, 16053.
(13) Mulliken, R. S. Electronic Population Analysis on LCAO−MO Molecular Wave Functions. I. *J. Chem. Phys.* **1955**, *23*, 1833−1840.
(14) Mulliken, R. S. Electronic Population Analysis on LCAO−MO Molecular Wave Functions. II. Overlap Populations, Bond Orders, and Covalent Bond Energies. *J. Chem. Phys.* **1955**, *23*, 1841−1846.
(15) Mulliken, R. S. Electronic Population Analysis on LCAO−MO Molecular Wave Functions. III. Effects of Hybridization on Overlap and Gross AO Populations. *J. Chem. Phys.* **1955**, *23*, 2338−2342.
(16) Mulliken, R. S. Electronic Population Analysis on LCAO−MO Molecular Wave Functions. IV. Bonding and Antibonding in LCAO and Valence-Bond Theories. *J. Chem. Phys.* **1955**, *23*, 2343−2346.
(17) Chang, H.; Harrison, J. F.; Kaplan, T. A.; Mahanti, S. D. Cluster Study of the Neutron-Scattering Form Factor for Antiferromagnetic $KNiF_3$ and NiO. *Phys. Rev. B* **1994**, *49*, 15753−15758.
(18) Bauschlicher, C. W., Jr.; Bagus, P. S. The Metal-Carbonyl Bond in $Ni(Co)_4$ and $Fe(Co)_5$: A Clear-Cut Analysis. *J. Chem. Phys.* **1984**, *81*, 5889−5898.
(19) Denning, R. G. Electronic Structure and Bonding in Actinyl Ions and Their Analogs. *J. Phys. Chem. A* **2007**, *111*, 4125−4143.
(20) Bagus, P. S.; Nelin, C. J.; Hrovat, D. A.; Ilton, E. S. Covalent Bonding in Heavy Metal Oxides. *J. Chem. Phys.* **2017**, *146*, 134706.
(21) Hernandez-Trujillo, J.; Bader, R. F. W. Properties of Atoms in Molecules: Atoms Forming Molecules. *J. Phys. Chem. A* **2000**, *104*, 1779−1794.
(22) Reed, A. E.; Weinstock, R. B.; Weinhold, F. Natural Population Analysis. *J. Chem. Phys.* **1985**, *83*, 735−746.
(23) Reed, A. E.; Weinhold, F. Natural Localized Molecular Orbitals. *J. Chem. Phys.* **1985**, *83*, 1736−1740.
(24) Saue, T.; Bast, R.; Gomes, A. S. P.; Jensen, H. J. A.; Visscher, L.; Aucar, I. A.; Di Remigio, R.; Dyall, K. G.; Eliav, E.; Fasshauer, E.; Fleig, T.; Halbert, L.; Hedegård, E. D.; Helmich-Paris, B.; Iliaš, M.; Jacob, C. R.; Knecht, S.; Laerdahl, J. K.; Vidal, M. L.; Nayak, M. K.; Olejniczak, M.; Olsen, J. M. H.; Pernpointner, M.; Senjean, B.; Shee, A.; Sunaga, A.; van Stralen, J. N. P. The Dirac Code for Relativistic Molecular Calculations. *J. Chem. Phys.* **2020**, *152*, 204104.
(25) Abragam, A.; Bleaney, B. *Electron Paramagnetic Resonance of Transition Ions*; Clarendon Press: Oxford, 1970.
(26) Levine, I. N. *Quantum Chemistry*; Prentice-Hall: Upper Saddle River, NJ, 2000.
(27) Visscher, L.; Visser, O.; Aerts, P. J. C.; Merenga, H.; Nieuwpoort, W. C. Relativistic Quantum Chemistry: The Molfdir Program Package. *Comput. Phys. Commun.* **1994**, *81*, 120−144.
(28) Bagus, P. S.; Ilton, E. S.; Nelin, C. J. The Interpretation of XPS Spectra: Insights into Materials Properties. *Surf. Sci. Rep.* **2013**, *68*, 273−304.
(29) Bagus, P. S.; Sousa, C.; Illas, F. Limitations of the Equivalent Core Model for Understanding Core-Level Spectroscopies. *Phys. Chem. Chem. Phys.* **2020**, *22*, 22617−22626.
(30) Bagus, P. S.; Ilton, E. S.; Nelin, C. J. Extracting Chemical Information from XPS Spectra: A Perspective. *Catal. Lett.* **2018**, *148*, 1785−1802.
(31) Saue, T.; Visscher, L.; Jensen, H. J. A.; Bast, R., with Contributions from Bakken, V.; Dyall, K. G.; Dubillard, S.; Ekström, U.; Eliav, E.; Enevoldsen, T.; Faßhauer, E.; Fleig, T.; Fossgaard, O.; Gomes, A. S. P.; Helgaker, T.; Henriksson, J.; Iliaš, M.; Jacob, C. R.; Knecht, S.; Komorovský, S.; Kullie, O.; Larsen, C. V.; Lærdahl, J. K.; Lee, Y. S.; Nataraj, H. S.; Norman, P.; Olejniczak, G.; Olsen, J.; Park, Y. C.; Pedersen, J. K.; Pernpointner, M.; Di Remigio, R.; Ruud, K.; Sałek, P.; Schimmelpfennig, B.; Sikkema, J.; Thorvaldsen, A. J.; Thyssen, J.; Van Stralen, J.; Villaume, S.; Visser, O.; Winther, T.; Yamamoto, S.; (See Http://Www.Diracprogram.Org), *Dirac, A Relativistic Ab Initio Electronic Structure Program*, Release Dirac14, 2014.
(32) Lefebvre-Brion, H.; Field, R. W. *Chapter 2—Basic Models*. In *The Spectra and Dynamics of Diatomic Molecules*; Lefebvre-Brion, H., Field, R. W., Eds.; Academic Press: San Diego, 2004, pp 61−86.
(33) Bagus, P. S.; Nelin, C. J.; Brundle, C. R.; Crist, B. V.; Ilton, E. S.; Lahiri, N.; Rosso, K. M. Main and Satellite Features in the Ni 2p Xps of Nio. *Inorg. Chem.* **2022**, *61*, 18077−18094.
(34) Bagus, P. S.; Nelin, C. J.; Brundle, C. R.; Lahiri, N.; Ilton, E. S.; Rosso, K. M. Analysis of the Fe 2p XPS for Hematite αFe_2O_3: Consequences of Covalent Bonding and Orbital Splittings on Multiplet Splittings. *J. Chem. Phys.* **2020**, *152*, 014704.
(35) Schaefer, H. F. *The Electronic Structure of Atoms and Molecules*; Addison-Wesley: Reading: Boston, 1972.
(36) Roos, B. O.; Taylor, P. R.; Sigbahn, P. E. A Complete Active Space Scf Method (CASSCF) Using a Density Matrix Formulated Super-Ci Approach. *Chem. Phys.* **1980**, *48*, 157−173.